Published in final edited form as:
*Pain*. 2010 February ; 148(2): 257. doi:10.1016/j.pain.2009.11.008.

# Exploring the brain in pain: activations, deactivations and their relation

**Jian Kong**[1,2,*], **Marco L Loggia**[1,2,5], **Carolyn Zyloney**[1], **Peichi Tu**[1], **Peter LaViolette**[1,2], and **Randy L Gollub**[1,2,3]

[1]Department of Psychiatry, Massachusetts General Hospital (MGH), Harvard Medical School, Charlestown, MA, USA

[2]MGH/MIT/HMS Athinoula A. Martinos Center for Biomedical Imaging, Charlestown MA, USA

[3]MGH/MIT CRC Biomedical Imaging Core, Charlestown, MA, USA

[4]Osher Institute, Harvard Medical School, Boston, MA, USA

[5]Department of Anesthesiology, Perioperative and Pain Medicine, Brigham and Women's Hospital, Harvard Medical School, Boston, Massachusetts, USA

## Abstract

The majority of neuroimaging studies on pain focus on the study of BOLD activations, and more rarely on *deactivations*. In this study, in a relatively large cohort of subjects (N=61), we assess: a) the extent of brain activation and deactivation during the application of two different heat pain levels (HIGH and LOW) and b) the relations between these two directions of fMRI signal change. Furthermore, in a subset of our subjects (N=12), we assess c) the functional connectivity of pain-activated or -deactivated regions during resting states. As previously observed, we find that pain stimuli induce intensity dependent (HIGH pain > LOW pain) fMRI signal increases across the pain matrix. Simultaneously, the noxious stimuli induce activity decreases in several brain regions, including some of the 'core structures' of the default network (DMN). In contrast to what we observe with the signal increases, the extent of deactivations is greater for LOW than HIGH pain stimuli. The functional dissociation between activated and deactivated networks is further supported by correlational and functional connectivity analyses. Our results illustrate the absence of a linear relationship between pain activations and deactivations, and therefore suggest that these brain signal changes underlie different aspects of the pain experience.

## Introduction

Over the last two decades, neuroimaging experiments have substantially increased our knowledge of how the brain processes pain, both in health and disease [2;36;43;44]. The vast majority of the studies published so far, however, predominantly focuses on brain activations, and tends to neglect brain *deactivations* (*i.e*., reductions in brain activity during exposure to



*Corresponding author: **Jian Kong**, Psychiatry Department, Massachusetts General Hospital, Building 149, 13th Street, Suite 2661, Charlestown, MA, 02129, Tel: 617-726-7893, Fax: 617-726-4078, kongj@nmr.mgh.harvard.edu

The authors have no conflicts of interest or competing financial interests to declare.

painful stimuli). Nonetheless, some studies indicate that an investigation of deactivations might yield a fuller understanding of central pain processing. For instance, Iannetti and colleagues [19] observed that, during central sensitization, nociceptive stimulation was associated with stronger and more extended occipital, frontal and temporal cortex deactivations compared to stimulation in normal states, and that the anti-hyperalgesic effect of gabapentin (a drug effective in neuropathic pain patients) was more strongly associated with a reduction in pain-evoked deactivations, than on its effect on activations. Thus, this and other studies suggest that deactivations might have an important role in chronic pain.

Gusnard and Raichle [16] suggested that two main categories of task-induced reductions of the brain activity can be observed in neuroimaging studies: dependent and independent from the nature of the task. The former may derive from mechanisms of cross-modal interaction which leads to the suppression, or 'gating', of information processing in areas that are not actively engaged in the performance of the task [11;17;20;26]. Selective attention can in fact differentially modulate brain activity underlying different primary sensory modalities, such that the processing of the attended information is facilitated, while the input of unattended sensory modalities is filtered out [11;17;20].

In addition to these task-specific reductions in regional brain activation, investigators have begun to realize that a very specific network of brain structures (medial prefrontal cortex (MPFC), posterior cingulate/retrosplenial cortex (PCC), inferior parietal lobule (IPL), lateral temporal cortex *(*LT) and hippocampal formation (HF) [4]) consistently displays task-induced activity reductions which are independent of the nature of the task [4;32;38;41]. This so-called 'default mode network' (DMN) may be involved in internally directed cognitive activity ('internal mentation hypothesis') and/or broad monitoring of the external environment in the absence of attention-demanding stimuli ('sentinel hypothesis') [4].

In the present study we took advantage of a relatively large dataset of subjects we had previously scanned (N=61) to systematically investigate fMRI signal increases and decreases during the application of two pain levels, and the correlations between the fMRI signal increase and decrease across different brain regions. In addition, we have also collected fMRI data during resting state from 12 of these subjects, on which we performed a functional connectivity analysis to further investigate spontaneous coherence in brain regions that showed significant fMRI signal changes during the heat pain administration.

## Material and Methods

In the present study, we pooled data from several experiments [22;24;25] from our lab. Although the original aims of these experiments were different (*i.e.*, to investigate the brain mechanisms of placebo, nocebo and acupuncture analgesia), each of these studies included two fMRI trials 'at baseline' (*i.e.*, in the absence of any experimental treatment) at the beginning of the fMRI scanning session, in which random heat pain stimuli of different intensity levels were applied on the right forearm. Since these baseline sessions were completely identical across studies, we believe that pooling these data together in order to achieve large statistical power is appropriate. Additional details on the experimental procedures which are specific to each individual study, but irrelevant for the present manuscript, will not be further discussed.

61 healthy right handed subjects were included in this study. All experiments were conducted with the written consent of each subject and approved by the Massachusetts General Hospital's Institutional Review Board.

## Procedures for the Delivery and Assessment of Noxious Thermal Stimuli

All subjects were recruited to participate in two behavioral testing sessions and one fMRI scanning session**.** Each session was separated by a minimum of three days. Calibrated thermal pain stimuli were delivered to the right medial aspect of the forearm using a TSA-2001 Thermal Sensory Analyzer with a 3 cm × 3 cm probe (Medoc Advanced Medical Systems, Rimat Yishai, Israel) running the COVAS software. All stimuli were initiated from a baseline resting temperature of 32 °C and increased to a target temperature. Each stimulus was presented for 12 seconds, including 2.5 seconds to ramp up towards the target temperature from baseline and 2.5 seconds to ramp back down to baseline, and the inter-stimulus interval ranged from 24 to 30 seconds.

The Gracely Sensory scale [14;15] was used following each heat pain stimulus to measure subjective pain ratings.

### Behavioral session 1

We used the first behavioral session to familiarize subjects with the rating scale and determine appropriate stimulus intensities using methods employed in our previous studies [10;21-24; 27]. Briefly, an ascending series of noxious heat stimuli (increasing by 1 °C per stimulus) was applied on two areas on the right distal volar forearm (adjacent to the wrist) in order to identify for each individual the temperatures eliciting subjective intensity ratings in the LOW pain range (~ 5; which corresponds to the '*weak*' label on the 0-20 Sensory Scale) and HIGH pain range (~ 15; '*strong*'). A random series of 8 noxious stimuli, including 4 HIGH and 4 LOW, was then presented on the same areas of the forearm. Temperatures were adjusted when necessary to ensure that each individual's subjective ratings of HIGH and LOW remained in the desired range. The final temperature settings were used in the following two sessions.

### Behavioral session 2

In order to assess the stability of the subjective ratings, the series of random heat pain stimuli was applied on the same region of the body once more in this session. To proceed in the study, subjects had to consistently rate the HIGH pain stimuli as being more painful (indicated by a higher score on the Sensory scale) than the LOW pain stimuli. Additionally, subjects had to report approximately equivalent ratings (i.e., with an average pain rating difference of less than 1.5 on the 0-20 Gracely Sensory scale) in this and the final series of the first testing session.

### fMRI session

The random heat pain series on the right forearm was then repeated a third time, in the fMRI scanner. Two random pain sequences were applied on the distal forearm while the subjects were instructed to focus on a small black fixation cross in the center of a screen in front of them. The cross turned red to cue the onset of each stimulus and then turned black again when the temperature returned to baseline (i.e., after 12 seconds). Next, after a delay of 4, 6 or 8 seconds, the Sensory Box Scale was displayed on the screen for 8 seconds, and subjects moved a cursor along the scale to indicate their subjective ratings. The interval between the end of the presentation of the rating scale and start of the delivery of the next pain stimulus ranged from 8 to 14 second, with an average of 12 seconds (Figure 1A).

In addition to the pain runs, one six-minute resting state scan was acquired for 12 subjects at the beginning of the scanning session. For this scan subjects' were instructed to close their eyes and relax for the duration of the scan.

### Behavioral Data Analysis

A paired t-test was performed to compare the subjective pain sensory ratings of HIGH pain and LOW pain.

### fMRI Data Acquisition and Analysis

Brain imaging was performed with a 3-axis gradient head coil in a 3 Tesla Siemens MRI System equipped for echo planar imaging (of the total 61 subjects, 26 subjects were scanned with an 3 Tesla head-only Siemens Allegra MRI System, the remaining 35 subjects were scanned with a 3 Tesla whole-body Siemens Trio MRI System, but scanning parameters remained consistent across the two systems. All 12 subjects with spontaneous fMRI were scanned with a 3 Tesla whole-body Siemens MRI System). Thirty axial interleaved slices (4 mm thick with 1 mm skip) parallel to the anterior and posterior commissure covering the whole brain were acquired with TR=2000 ms, TE=40 ms, flip angle= 90° , and a 3.13 × 3.13 mm in-plane spatial resolution. A high-resolution 3D MPRAGE sequence for anatomic localization was also collected.

Pre-processing and statistical analysis were performed using SPM2 software (Wellcome Department of Cognitive Neurology, London, UK). Pre-processing included motion correction, spatial normalization to the MNI template, spatial smoothing with an 8 mm Gaussian kernel, and high-pass temporal filtering (cut-off 128s). The fMRI signal was then modeled by using the general linear model (GLM). Explanatory variables included in the model were LOW pain, HIGH pain, rating period and baseline. The regressors were modeled using a boxcar function convolved with the SPM hemodynamic response function. Group analysis was performed using a random-effects model, generating statistical maps of increased and decreased brain activity in response to heat stimuli. The following contrasts were computed for each subject: 'HIGH pain vs. baseline', 'LOW pain vs. baseline' and 'HIGH pain vs. LOW pain'. Given the relatively large sample size and robust fMRI signal changes, we decided to use a stringent criterion to determine statistical significance, with a voxel-wise threshold of $p = 0.05$ corrected (family-wise error, FWE), and a minimum cluster extent of 10 contiguous voxels, for all comparisons. In addition, to explore any potential gender differences, we also performed a two sample t-test between the male and female subjects on brain activations associated with HIGH and LOW pain separately. For this analysis, the voxel-wise threshold was set at $p$=0.001, uncorrected for 20 contiguous voxels.

In a subsequent analysis, the β values associated with the activity of several brain regions displaying significant pain-evoked activity changes (in either direction) for both LOW and HIGH pain vs. baseline were extracted using a 3 mm sphere around the peak of activation, and then correlated with each other. In order to keep the number of statistical comparisons to a minimum, we included in this correlational analysis only areas that were significantly activated or deactivated in the (LOW or HIGH) 'pain vs baseline' contrasts, and that belonged to one of the following categories: a) 'reliable pain regions' (i.e., the four cortical regions most reliably activated in fMRI pain studies: ACC, insula, S1 and S2 [2]); b) 'reliable DMN regions' (i.e., the brain regions of the default network which are most consistently deactivated in imaging studies: medial prefrontal cortex, posterior cingulate/retrosplenial cortex, inferior parietal lobule and lateral temporal cortex [4]) or c) 'strongly deactivated regions' (i.e., areas displaying the pain-related deactivations with the highest peak z-value during either LOW or HIGH pain: left and right occipital gyri and right M1/S1). This allowed us to investigate the correlation between the activity of 1) areas displaying fMRI signal increases; 2) areas displaying fMRI signal decreases; 3) activated and deactivated areas; 4) corresponding (homologous) areas in the two hemispheres, and 5) the lateral and medial pain networks (represented by S2 and ACC, respectively). Since the application of HIGH and LOW pain evoked activity changes in overlapping but not entirely identical regions (see Results), a Pearson correlation analysis was

carried for each of the two pain conditions separately. For each pain level, the BOLD signal from each of the 11 ROIs selected according to the criteria specified above was cross correlated. Therefore, a total of 55 correlations were performed per pain level. To correct for multiple tests, the Bonferroni correction was applied, and the resulting corrected α value of 0.0009 (=0.05/55) was adopted in this analysis. The average % signal change from the 3mm sphere was extracted for illustrative purposes for some representative regions, using the MarsBaR toolbox for SPM. Throughout the text and tables, coordinates refer to the MNI space.

### Functional Connectivity Analysis

To further investigate the functional correlation between brain regions displaying pain-evoked activity changes, pain (de)activated were used as seed regions for a functional connectivity study of the resting state data (n=12) collected at the beginning of the fMRI scan session. Methods for this functional connectivity analysis were similar to those employed in previous studies [1;13;22;28;46].

Briefly, functional data were first preprocessed to decrease image artifacts and between-slice timing differences, and to eliminate differences in odd/even slice intensity. Rigid body translations and rotations were used to reduce within and across-run head movement. Data were re-sampled to 2mm isotropic voxels after transforming anatomical and functional data to the MNI atlas space.

The functional connectivity analysis required the application of a low-pass temporal filter, which removed constant offsets and linear trends over each run while retaining frequencies below 0.083 Hz [28]. Spatial smoothing was performed using a 6mm Gaussian kernel. Variables that were simultaneously regressed included movement parameters, whole brain signal, lateral ventricle mean signals, deep white matter ROI signal, and the first temporal derivative of each time course. From the resulting time series, correlation maps between seed regions and all voxels across the whole brain were computed. The 3-mm spherical seed regions for the functional connectivity analysis were positioned in brain areas selected according to the same criteria adopted for the correlational analyses mentioned above (i.e., among the areas showing significant pain-related changes, only those belonging to ‘reliable pain regions’, ‘reliable DMN regions’ or ‘strongly deactivated regions’ were included); for each of these areas, the right or left hemisphere was chosen depending on which side displayed the stronger activations or deactivations. Finally, within the selected areas, the seed regions were centered at the level of the peak coordinates determined by either the ‘High-pain vs. baseline’ or ‘Low-pain vs. baseline’ contrasts, depending on which contrast produced the most and largest activations or deactivations. The regions and peak coordinates identified according to these criteria are shown in Table 6.

This analysis produced coefficients for each seed-voxel correlation. Fisher’s r-to-z transformation was used to convert correlation maps into z maps. Group effects were tested with a random-effect analysis using a one sample t-test. The threshold was set at voxel-wise $p<0.001$ uncorrected for 20 contiguous voxels.

## Results

### Subjects

In total, the data from 61 healthy normal right handed subjects (mean age ± SD: 26.6 ± 4.7) were included in this study. Of these subjects, 33 were females (mean age: 25.6 ± 2.9) and 28 were males (mean age: 27.8 ± 6.0). No significant age differences were observed between genders (p = 0.08). The resting state scan was acquired in 12 (7 females; mean age: 27.1 ± 3.7) of these 61 subjects.

### Subjective Ratings of Pain

The subjective pain sensory ratings (mean ± SD) for the HIGH and LOW pain stimuli were 14 ± 1.9 (ranging from 9.8 to 18.4) and 4.9 ± 2.5 (ranging from 1.1 to 11.5) respectively. A paired t test showed that there was a significant difference ($p < 0.0001$) between the two levels of pain. The average pain sensory ratings for female subjects were 5.0± 2.6 and 14.3 ± 2.0 for LOW and HIGH pain stimuli respectively; those for male subjects were 4.8± 2.4 and 13.7 ± 1.7; we observed no significant rating differences between genders for both high pain ($p=0.70$) and low pain (0.22) stimuli.

### fMRI results

**LOW pain vs. baseline—**The administration of LOW pain evoked fMRI signal increases in the bilateral insula, medial frontal gyrus, left S2, cerebellum, right inferior / middle frontal gyrus, and inferior parietal lobule (Figure 1b; Table 1).

Asides from activity increases in these areas, the application of LOW pain stimuli also produced significant widespread fMRI signal decreases in areas such as the bilateral medial frontal gyrus / ACC, occipital / middle temporal gyrus, precuneus, midcingulate, posterior cingulate cortex / retrosplenial cortex, parahippocampus / hippocampus, uncus, superior frontal gyrus, posterior thalamus, hypothalamus and cerebellum, motor / premotor cortex, left precentral gyrus, and right stratum (Figure 1c; Table 1). Interestingly, the voxels significantly deactivated during pain (n=33834) greatly outnumbered those significantly activated (n=3866).

**HIGH pain vs. baseline—**Compared to baseline, HIGH pain stimuli elicited activations in bilateral insula / operculum / inferior frontal gyrus (47) / thalamus / striatum / superior & middle temporal gyrus, ACC / medial frontal gyrus, S2, brainstem, cerebellum, left S1 / M1, middle frontal gyrus, right inferior / middle frontal gyrus. HIGH pain-evoked deactivations were observed in bilateral medial prefrontal cortex / ACC, post cingulate cortex / precuneus, lateral occipital gyrus, left superior frontal gyrus, right superior parietal lobule and S1 / M1 (Figure 1b,c; Table 2).

In contrast to the results obtained for the LOW pain stimuli, the voxels significantly deactivated during HIGH pain (2112) were greatly outnumbered by those significantly activated (37559).

The average time course of the BOLD signal within some representative pain-activated and –deactivated regions can be observed in Figure 2.

**HIGH pain vs. LOW pain—**Compared to LOW pain stimulation, HIGH pain stimuli evoked significantly higher fMRI signal increases in a number of brain areas (Figure 1d; Table 3). These regions include bilateral insula / operculum / inferior frontal gyrus (47) / thalamus / striatum / superior / middle / inferior temporal gyrus, ACC / medial frontal gyrus, middle temporal gyrus, S2, cuneus, PAG, cerebellum, M1, left S1, middle frontal gyrus, calcarine sulcus / cuneus / middle occipital gyrus, medial prefrontal cortex, right premotor cortex, and superior frontal gyrus. Since a positive BOLD signal in the 'HIGH vs. LOW' contrast could be either due to stronger activations or to reduced deactivations in the HIGH pain condition, these areas were masked with the voxels found statistically deactivated during the application of LOW pain (i.e., those which displayed a stronger BOLD signal at baseline, than during LOW pain). This allowed us to identify a subset of brain areas displaying reduced deactivations (or activations as opposed to deactivations) during HIGH pain, as compared to LOW pain. These regions included bilateral medial prefrontal cortex / paracentral lobule (6 / 4), midcingulate / posterior cingulate cortex / precunus (23/31), parietal lobule (40), precentral gyrus (4 / 6), cuneus (18), thalamus, cerebellum; left middle temporal gyrus (21), inferior temporal gyrus (20), and right striatum (Figure 1e).

## Gender comparison

The gender comparison revealed that male subjects exhibited stronger BOLD signals in pain-activated regions, for both LOW pain (left insula / operculum) and HIGH pain (bilateral insula / operculum, S2, thalamus, rostral and dorsal ACC, left brain stem, MPFC, and right DLPFC). There were no regions in which the BOLD signal was stronger for female subjects for either HIGH or LOW pain. Since the areas in which $BOLD_{males} > BOLD_{females}$ did not overlap with the pain-deactivated areas described above, male subjects appeared to exhibit stronger pain-related activations than female subjects, but similar deactivations.

### Correlational analysis

The results of this analysis (brain regions, peak coordinate, r and p values) are presented in Table 4 and Table 5 separately.

### Pain-activated areas

For both pain levels, fMRI signal increases were in general significantly correlated in all the 'reliable pain areas' we found activated.

### Pain-deactivated areas

fMRI signal decreases in pain-deactivated areas belonging to the default network (PCC/precuneus and MPFC for both LOW and HIGH pain, and bilateral lateral temporal cortex for LOW pain only) were significantly correlated with each other. Among the other pain-deactivated regions, the left and right lateral occipital brain regions were significantly correlated with each other in both pain levels, but their correlation with the pain-deactivated areas of the default network depended on the intensity of pain. During LOW pain, right occipital gyrus, but not left, showed significant correlation with PCC, precuneus, OMPFC and bilateral lateral temporal cortex. During HIGH pain, however, both left and right occipital gyri were significantly correlated with PCC (and not with other DMN pain-deactivated areas).

### Pain-activated Vs Pain-deactivated areas

No significant correlations were observed between pain-evoked activations and deactivations, except between the pain-activated right S1 and the pain-deactivated left S1/M1 and left and right occipital cortex during HIGH pain.

### Functional Connectivity Analysis

The results from the functional connectivity analysis of the twelve subjects' resting state scans are shown for each of the selected brain seed regions in Figure 3. Overall, brain regions displayed symmetric activity on the two sides of the brain; for instance, a clear synchronous activity was observed between left and right insula, as well as between left and right somatosensory cortices, or left and right lateral temporal cortices.

### Resting state in pain-activated areas

Spontaneous activity of the ACC was significantly synchronized with that of several other brain regions, such as the MPFC, ACC, bilateral anterior / middle insula, thalamus, caudate nucleus, lateral prefrontal cortex and cerebellum. When we used left S1 as a seed region, synchronized activity was observed at the level of bilateral s1/M1, MPFC / mid-cingulate cortex, posterior insula / S2, and occipital cortex. Using left S2 as a seed region, significant associations were observed with bilateral S2, insula / operculum, ACC, left S1 and lateral prefrontal gyrus. The functional connectivity map for the right anterior insula included bilateral AI / operculum, ACC, mid-cingulate cortex, caudate, globus pallidus, thalamus, cerebellum and brain stem.

### Resting state in pain-deactivated areas

Among the seed regions showing fMRI signal decreases during administration of pain, vMPFC and PCC showed similar functional connectivity networks, including vMPFC, dMPFC, posterior cingulate/retrosplenial cortex, inferior parietal lobule / angular gyrus, lateral temporal cortex, hippocampus and cerebellum. The right lateral temporal cortex showed less robust connectivity with other areas of the default network, as well as with additional regions such as the lateral and medial occipital cortex. Finally, the association network of right occipital lateral gyrus was found to be quite local, including bilateral lateral and medial occipital cortex, and left lateral temporal cortex.

## Discussion

In this study, we investigated fMRI signal changes evoked by heat pain in a relatively large cohort of subjects. As expected, we found that the application of noxious stimuli produces not only activations within the 'pain matrix' [2;27;36;44], but also widespread deactivations. Since negative BOLD responses have been shown to correlate with decreases in neuronal activity [34;40], and therefore do not merely represent a vascular epiphenomenon, the results from this and other studies appear to suggest that a large network of areas in the brain decreases its activity during pain. These fMRI signal decreases were observed in so-called 'core regions of the default network' [4], such as bilateral MPFC, posterior cingulate cortex / precuneus, parahippocampus / hippocampus and lateral temporal cortex, as well as in brain regions not traditionally associated with the DMN, such as lateral occipital gyri, premotor area, superior frontal gyrus and contralateral S1 / M1.

The DMN is a widespread network of brain structures which appears to be engaged when individuals are left to think to themselves undisturbed, and was shown to reduce its activity during the execution of a wide variety of goal-oriented behaviors [4;32;38;41]. Although its specific functions are currently under debate, two leading hypotheses have been recently formulated [4]. According to the 'sentinel hypothesis,' this network would support broad monitoring of the external environment in the absence of attention-demanding stimuli. Our data do not seem to support this hypothesis. In fact, if the pain-related deactivations were due to the interruption of the broad monitoring of the external environment, then increasing levels of pain would have to be associated with increasing deactivations. To our surprise, however, LOW pain stimuli induced deactivations in a much larger network of brain regions than HIGH pain (Figure 1e).

A second hypothesis, the 'internal mentation hypothesis', poses that the DMN would support internally directed cognitive activity that is largely detached from the external world, and specifically have a role in 'constructing dynamic mental simulations based on personal past experiences such as used during remembering, thinking about the future, and generally when imagining alternative perspectives and scenarios to the present' [4]. Our observation that higher pain is associated with lower deactivations might be compatible with the this hypothesis: in fact, due to the threat that intensely painful stimuli pose to the organism, it is possible that high pain leads subject to instinctively mentally explore 'alternative scenarios' in order to prepare for an escape from pain. This exploration of potential solutions to the current threat might partially counteract the DMN inhibition induced by the incoming stimulation, particularly for intensely painful stimuli. Alternatively, the observed differences in the extent and magnitude of deactivations might relate to differences in the cognitive load across stimulus intensities. In fact, as we have previously reported [27], evaluating the painfulness of a stimulus is more effortful, and requires a more extensive activation of pain evaluative networks, for mild to moderate stimuli, than for high intensity stimuli.

Although most imaging studies published to date focus on BOLD activations, pain-induced fMRI or PET deactivations have been reported [3;5-8;12;18;[19,29-31,33,35,37];42;45;47;48]. In several of these studies the deactivations were either simply interpreted in terms of cross-modal inhibition, or briefly reported and not further discussed. Some others, however, indicate that deactivations might play a more prominent role in central processing of pain (e.g., [19]). Interestingly, some studies have reported stronger deactivations with increasing pain [6;37], in brain areas where we observed that HIGH pain was associated with lesser deactivation than LOW pain (e.g., posterior cingulate/precuneus or medial prefrontal areas). We currently have no hypotheses to explain this apparent discrepancy, and future experiments will need to clarify this issue. However, by illustrating that activations and deactivations can, at least in some circumstances, have a different relation with stimulus intensity, our results suggest that activations and deactivations might underlie different aspects of the pain experience.

When we compared the fMRI responses to LOW and HIGH pain in male and female subjects, we observed that males showed stronger activations than females in several areas (LOW pain: left insula / operculum; HIGH pain: bilateral insula / operculum, S2, thalamus, rostral and dorsal ACC, left brain stem, MPFC, and right DLPFC). These results are in line with other studies showing generally stronger pain related activations in male subjects [3;9]. However we did not observe any gender differences in deactivations, whereas stronger pain-related deactivations in females have been previously reported [3;33].

In support of the functional dissociation between BOLD increases and decreases are the results of the correlational and functional connectivity analyses. The correlational analysis on the fMRI signals of different brain regions during different pain levels showed that 1) the activity of regions showing fMRI signal increases were in general significantly correlated; 2) the activity of pain-activated regions was not correlated with that pain-deactivated regions 3) within the regions showing fMRI signal decreases, those traditionally classified as belonging to DMN (PCC, vMPFC, dMPFC, PCC/precuneus, bilateral lateral temporal cortex) were significantly correlated, whereas 4) the left and right lateral occipital brain regions were significantly correlated with each other, but their relation with other deactivated areas depended on the level of painful stimulation. The latter observations appear to indirectly support the view that there are different mechanisms underlying fMRI signal decrease in pain perception processes.

To further investigate the functional connection between different brain regions observed in fMRI group analysis, we performed a functional connectivity analysis on the resting state data collected at the beginning of the fMRI scan session in a subset of our subjects. Four brain regions showing fMRI signal increase were selected: ACC, left S1, right insula and S2. Traditionally, it is believed that S1 and S2 belong to lateral pain system, whereas ACC and anterior insula belong to medial pain system. Our results seem to provide some support to this notion. In fact, S1 displayed synchronous activity with bilateral S1/M1, mid-cingulate cortex, posterior insula / S2, and occipital cortex, but not with ACC, one of the brain regions most consistently associated with affective dimension of pain [39]. Placing a seed in the left S2 also achieved similar results. When we used ACC as the seed region, significant synchronous activity was observed in several brain regions including bilateral ACC, mid-cingulate cortex, bilateral anterior / middle insula, thalamus, caudate, orbital PFC, LPFC, cerebellum, but not in S1 or S2. Similar results were obtained with the anterior insula.

Among the regions showing fMRI signal decrease during administration of pain, several core areas of the default network, such as the vMPFC, PCC and left lateral temporal cortex, displayed synchronous activity at rest. The functional connectivity maps for areas outside the DMN, however, appeared rather different from that of DMN: for instance, we observed that the activity of the right lateral occipital gyrus was significantly synchronous with that of

bilateral lateral and medial occipital cortex, and left lateral temporal cortex. These results, along with those of the correlational analyses, suggest functional dissociation between lateral occipital cortex and other regions deactivated during painful stimulation, possibly supporting the notion that the mechanisms behind deactivations within and outside the default network might be of different nature (e.g., task-dependant vs task-independent; [16].

In conclusion, we report that pain stimuli induce robust, widespread, intensity dependent (HIGH pain > LOW pain) fMRI signal increases across the pain matrix. In addition, the noxious stimuli induce a simultaneous decrease in activation in several brain regions, including some of the 'core structures' of the DMN. In contrast to what we observe with the signal increases, the extent and magnitude of brain deactivation is greater for LOW than HIGH pain stimuli. Furthermore, correlation analyses indicate that the activity of areas displaying pain-evoked changes in the same direction is highly correlated, though there are no significant correlations between brain activations and deactivations. The functional dissociation between activated and deactivated networks is further supported by functional connectivity analyses, which show that spontaneous activity fluctuations are significantly correlated across areas displaying pain-induced changes of the same direction, but not of the opposite direction. Since our results show the absence of a linear relationship between pain-induced activations and deactivations, we propose that these brain signal changes may underlie different aspects of the pain experience.

## Acknowledgments

Funding and support for this study came from: KO1AT003883 and R21AT004497 to Jian Kong, R21AT00949 to Randy Gollub, NIH (NCCAM) PO1-AT002048 to Bruce Rosen, M01-RR-01066 and UL1 RR025758-01 for Clinical Research Center Biomedical Imaging Core from National Center for Research Resources (NCRR), P41RR14075 for Center for Functional Neuroimaging Technologies from NCRR and the MIND Research Network, DE-FG03-99ER62764 to Bruce Rosen.

## References

[1]. Andrews-Hanna JR, Snyder AZ, Vincent JL, Lustig C, Head D, Raichle ME, Buckner RL. Disruption of large-scale brain systems in advanced aging. Neuron 2007;56(5):924–935. [PubMed: 18054866]

[2]. Apkarian AV, Bushnell MC, Treede RD, Zubieta JK. Human brain mechanisms of pain perception and regulation in health and disease. Eur J Pain 2005;9(4):463–484. [PubMed: 15979027]

[3]. Berman SM, Naliboff BD, Suyenobu B, Labus JS, Stains J, Bueller JA, Ruby K, Mayer EA. Sex differences in regional brain response to aversive pelvic visceral stimuli. Am J Physiol Regul Integr Comp Physiol 2006;291(2):R268–276. [PubMed: 16614061]

[4]. Buckner RL, Andrews-Hanna JR, Schacter DL. The brain's default network: anatomy, function, and relevance to disease. Ann N Y Acad Sci 2008;1124:1–38. [PubMed: 18400922]

[5]. Coghill RC, Sang CN, Berman KF, Bennett GJ, Iadarola MJ. Global cerebral blood flow decreases during pain. Journal of Cerebral Blood Flow & Metabolism 1998;18(2):141–147. [PubMed: 9469155]

[6]. Coghill RC, Sang CN, Maisog JM, Iadorola MJ. Pain intensity processing within the human brain: a bilateral, distributed mechanism. Journal of Neurophysiology 1999;82:1934–1943. [PubMed: 10515983]

[7]. Derbyshire SW, Jones AK. Cerebral responses to a continual tonic pain stimulus measured using positron emission tomography. Pain 1998;76(12):127–135. [PubMed: 9696465]

[8]. Derbyshire SW, Jones AK, Gyulia F, Clark S, Townsend D, Firestone LL. Pain processing during three levels of noxious stimulation produces differential patterns of central activity. Pain 1997;73:431–445. [PubMed: 9469535]

[9]. Derbyshire SW, Nichols TE, Firestone L, Townsend DW, Jones AK. Gender differences in patterns of cerebral activation during equal experience of painful laser stimulation. J Pain 2002;3(5):401–411. [PubMed: 14622744]

[10]. Dougherty DD, Kong J, Webb M, Bonab AA, Fischman AJ, Gollub RL. A combined [11C] diprenorphine PET study and fMRI study of acupuncture analgesia. Behav Brain Res 2008;193(1): 63–68. PMCID: PMC2538486. [PubMed: 18562019]

[11]. Drevets WC, Raichle ME. Reciprocal suppression of regional cerebral blood flow during emotional versus higher cognitive processes: Implicaitons for interactions between emotion and cognition. Cognition and emotion 1998;12(3):352–385.

[12]. Dunckley P, Wise RG, Aziz Q, Painter D, Brooks J, Tracey I, Chang L. Cortical processing of visceral and somatic stimulation: differentiating pain intensity from unpleasantness. Neuroscience 2005;133(2):533–542. [PubMed: 15896917]

[13]. Fox MD, Snyder AZ, Vincent JL, Corbetta M, Van Essen DC, Raichle ME. The human brain is intrinsically organized into dynamic, anticorrelated functional networks. Proc Natl Acad Sci U S A 2005;102(27):9673–9678. [PubMed: 15976020]

[14]. Gracely RH, McGrath PA, Dubner R. Ratio scales of sensory and affective verbal pain descriptors. Pain 1978;5:5–18. [PubMed: 673440]

[15]. Gracely RH, McGrath PA, Dubner R. Validity and sensitivity of ratio scales of sensory and affective verbal pain descriptors: manipulation of affect by diazepam. Pain 1978;5:19–29. [PubMed: 673439]

[16]. Gusnard DA, Raichle ME. Searching for a baseline: functional imaging and the resting human brain. Nat Rev Neurosci 2001;2(10):685–694. [PubMed: 11584306]

[17]. Haxby JV, Horwitz B, Ungerleider LG, Maisog JM, Pietrini P, Grady CL. The functional organization of human extrastriate cortex: a PET-rCBF study of selective attention to faces and locations. J Neurosci 1994;14(11 Pt 1):6336–6353. [PubMed: 7965040]

[18]. Hsieh JC, Stahle-Backdahl M, Hagermark O, Stone-Elander S, Rosenquist G, Ingvar M. Traumatic nociceptive pain activates the hypothalamus and the periaqueductal gray: a positron emission tomography study. Pain 1996;64(2):303–314. [PubMed: 8740608]

[19]. Iannetti GD, Zambreanu L, Wise RG, Buchanan TJ, Huggins JP, Smart TS, Vennart W, Tracey I. Pharmacological modulation of pain-related brain activity during normal and central sensitization states in humans. Proc Natl Acad Sci U S A 2005;102(50):18195–18200. [PubMed: 16330766]

[20]. Kawashima R, O'Sullivan BT, Roland PE. Positron-emission tomography studies of cross-modality inhibition in selective attentional tasks: closing the "mind's eye". Proc Natl Acad Sci U S A 1995;92 (13):5969–5972. [PubMed: 7597062]

[21]. Kong J, Fufa DT, Gerber AJ, Rosman IS, Vangel MG, Gracely RH, Gollub RL. Psychophysical outcomes from a randomized pilot study of manual, electro, and sham acupuncture treatment on experimentally induced thermal pain. J Pain 2005;6(1):55–64. [PubMed: 15629419]

[22]. Kong J, Gollub RL, Polich G, Kirsch I, Laviolette P, Vangel M, Rosen B, Kaptchuk TJ. A functional magnetic resonance imaging study on the neural mechanisms of hyperalgesic nocebo effect. J Neurosci 2008;28(49):13354–13362. PMCID: PMC2649754. [PubMed: 19052227]

[23]. Kong J, Gollub RL, Rosman IS, Webb JM, Vangel MG, Kirsch I, Kaptchuk TJ. Brain activity associated with expectancy-enhanced placebo analgesia as measured by functional magnetic resonance imaging. J Neurosci 2006;26(2):381–388. [PubMed: 16407533]

[24]. Kong J, Kaptachuk TJ, Polich G, Kirsch IV, angel M, Zyloney C, Rosen B, Gollub R. Expectancy and treatment interactions: A dissociation between acupuncture analgesia and expectancy evoked placebo analgesia. Neuroimage 2009;45:940–949. NIHMSID #114915. [PubMed: 19159691]

[25]. Kong J, Kaptchuk TJ, Polich G, Kirsch I, Vangel M, Zyloney C, Rosen B, Gollub RL. An fMRI study on the interaction and dissociation between expectation of pain relief and acupuncture treatment. Neuroimage 2009;47(3):1066–1076. PMID: 19501656. [PubMed: 19501656]

[26]. Kong J, Kaptchuk TJ, Webb JM, Kong JT, Sasaki Y, Polich GR, Vangel MG, Kwong K, Rosen B, Gollub RL. Functional neuroanatomical investigation of vision-related acupuncture point specificity--a multisession fMRI study. Hum Brain Mapp 2009;30(1):38–46. [PubMed: 17990299]

[27]. Kong J, White NS, Kwong KK, Vangel MG, Rosman IS, Gracely RH, Gollub RL. Using fMRI to dissociate sensory encoding from cognitive evaluation of heat pain intensity. Hum Brain Mapp 2006;27(8):715–721. [PubMed: 16342273]

[28]. Krienen FM, Buckner RL. Segregated Fronto-Cerebellar Circuits Revealed by Intrinsic Functional Connectivity. Cereb Cortex. 2009

[29]. Kupers RC, Svensson P, Jensen TS. Central representation of muscle pain and mechanical hyperesthesia in the orofacial region: a positron emission tomography study. Pain 2004;108(3):284–293. [PubMed: 15030948]

[30]. Lui F, Duzzi D, Corradini M, Serafini M, Baraldi P, Porro CA. Touch or pain? Spatio-temporal patterns of cortical fMRI activity following brief mechanical stimuli. Pain 2008;138(2):362–374. [PubMed: 18313223]

[31]. May A, Kaube H, Buchel C, Eichten C, Rijntjes M, Juptner M, Weiller C, Diener HC. Experimental cranial pain elicited by capsaicin: a PET study. Pain 1998;74(1):61–66. [PubMed: 9514561]

[32]. Mazoyer B, Zago L, Mellet E, Bricogne S, Etard O, Houde O, Crivello F, Joliot M, Petit L, Tzourio-Mazoyer N. Cortical networks for working memory and executive functions sustain the conscious resting state in man. Brain Res Bull 2001;54(3):287–298. [PubMed: 11287133]

[33]. Moulton EA, Keaser ML, Gullapalli RP, Maitra R, Greenspan JD. Sex differences in the cerebral BOLD signal response to painful heat stimuli. Am J Physiol Regul Integr Comp Physiol 2006;291 (2):R257–267. [PubMed: 16601264]

[34]. Pasley BN, Inglis BA, Freeman RD. Analysis of oxygen metabolism implies a neural origin for the negative BOLD response in human visual cortex. Neuroimage 2007;36(2):269–276. [PubMed: 17113313]

[35]. Peyron R, Garcia-Larrea L, Gregoire M, Costes N, Convers P, Lavenne F, Mauguiere F, Michel D, Laurent B. Haemodynamic brain responses to acute pain in humans: sensory and attentional networks. Brain 1999;122:1765–1779. [PubMed: 10468515]

[36]. Peyron R, Laurent B, Garcia-Larrea L. Functional imaging of brain responses to pain. A review and meta-analysis (2000). Neurophysiol Clin 2000;30:263–288. [PubMed: 11126640]

[37]. Porro CA, Cettolo V, Francescato MP, Baraldi P. Temporal and intensity coding of pain in human cortex. J Neurophysiol 1998;80(6):3312–3320. [PubMed: 9862924]

[38]. Raichle ME, MacLeod AM, Snyder AZ, Powers WJ, Gusnard DA, Shulman GL. A default mode of brain function. Proc Natl Acad Sci U S A 2001;98(2):676–682. [PubMed: 11209064]

[39]. Rainville P, Duncan GH, Price DD, Carrier B, Bushnell MC. Pain affect encoded in human anterior cingulate but not somatosensory cortex. Science 1997;277:968–971. [PubMed: 9252330]

[40]. Shmuel A, Augath M, Oeltermann A, Logothetis NK. Negative functional MRI response correlates with decreases in neuronal activity in monkey visual area V1. Nat Neurosci 2006;9(4):569–577. [PubMed: 16547508]

[41]. Shulman GL, Fiez JA, Corbetta M, Buckner RL, Miezin FM, Raichle M, Peterson SE. Common blood flow changes across visual tasks: II. decreases in cerebral cortex. J Cognitive Neurosci 1997;9 (5):648–663.

[42]. Svensson P, Minoshima S, Beydoun A, Morrow TJ, Casey KL. Cerebral processing of acute skin and muscle pain in humans. J Neurophysiol 1997;78(1):450–460. [PubMed: 9242293]

[43]. Tracey I. Nociceptive processing in the human brain. Curr Opin Neurobiol 2005;15(4):478–487. [PubMed: 16019203]

[44]. Tracey I, Mantyh PW. The cerebral signature for pain perception and its modulation. Neuron 2007;55(3):377–391. [PubMed: 17678852]

[45]. van Oudenhove L, Vandenberghe J, Dupont P, Geeraerts B, Vos R, Bormans G, van Laere K, Fischler B, Demyttenaere K, Janssens J, Tack J. Cortical deactivations during gastric fundus distension in health: visceral pain-specific response or attenuation of ‘default mode’ brain function? A H2 15O-PET study. Neurogastroenterol Motil 2009;21(3):259–271. [PubMed: 19019011]

[46]. Vincent JL, Patel GH, Fox MD, Snyder AZ, Baker JT, Van Essen DC, Zempel JM, Snyder LH, Corbetta M, Raichle ME. Intrinsic functional architecture in the anaesthetized monkey brain. Nature 2007;447(7140):83–86. [PubMed: 17476267]

[47]. Vogt BA, Derbyshire S, Jones AK. Pain processing in four regions of human cingulate cortex localized with co-registered PET and MR imaging. Eur J Neurosci 1996;8(7):1461–1473. [PubMed: 8758953]

[48]. Yelle MD, Oshiro Y, Kraft RA, Coghill RC. Temporal filtering of nociceptive information by dynamic activation of endogenous pain modulatory systems. J Neurosci 2009;29(33):10264–10271. [PubMed: 19692600]

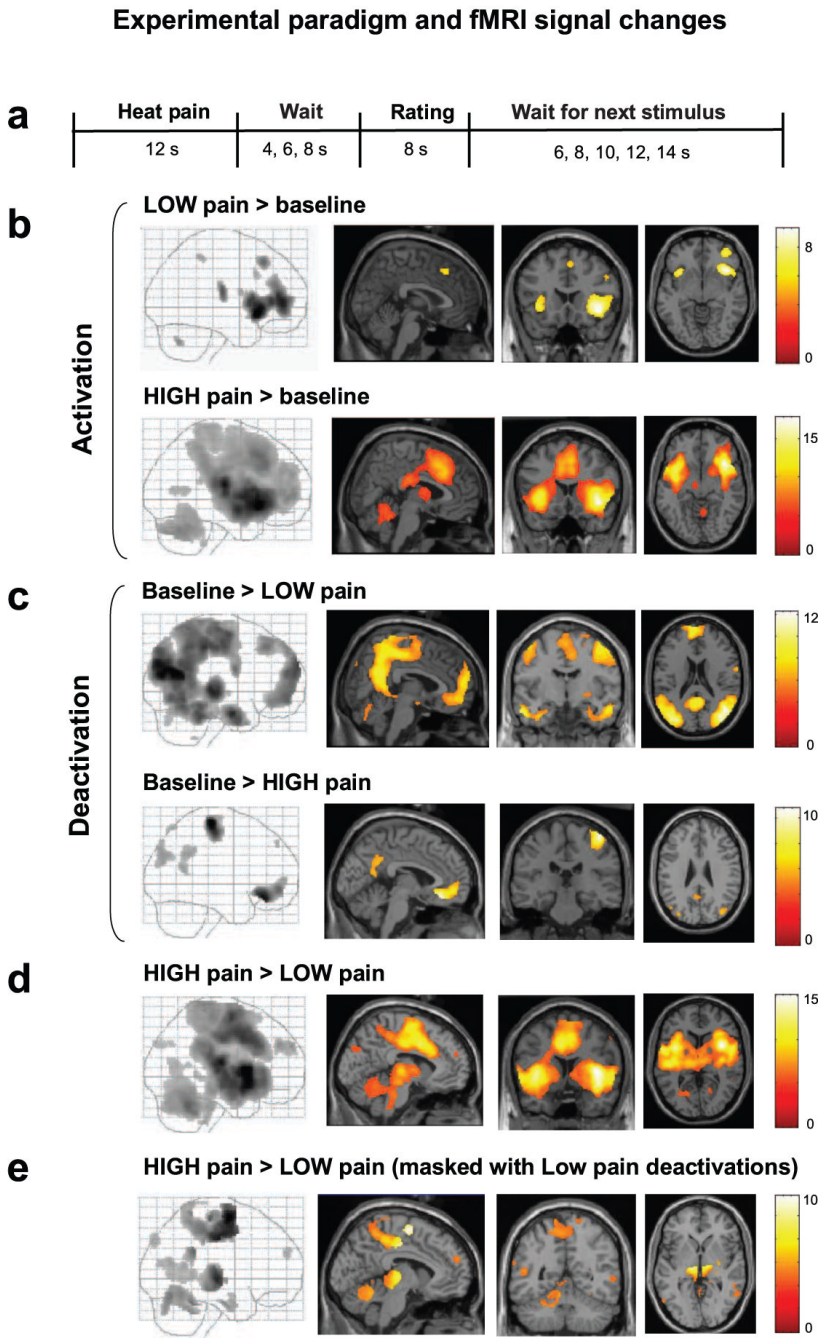


**Figure 1. Experimental paradigm (a) and fMRI signal increases and decreases evoked by LOW and HIGH pain stimuli (b-e)**

Panel **d** shows the areas where HIGH pain induced higher BOLD signal than LOW, and panel **e** highlights the areas displaying reduced deactivations (or activations as opposed to deactivations) during HIGH pain, compared to LOW pain.

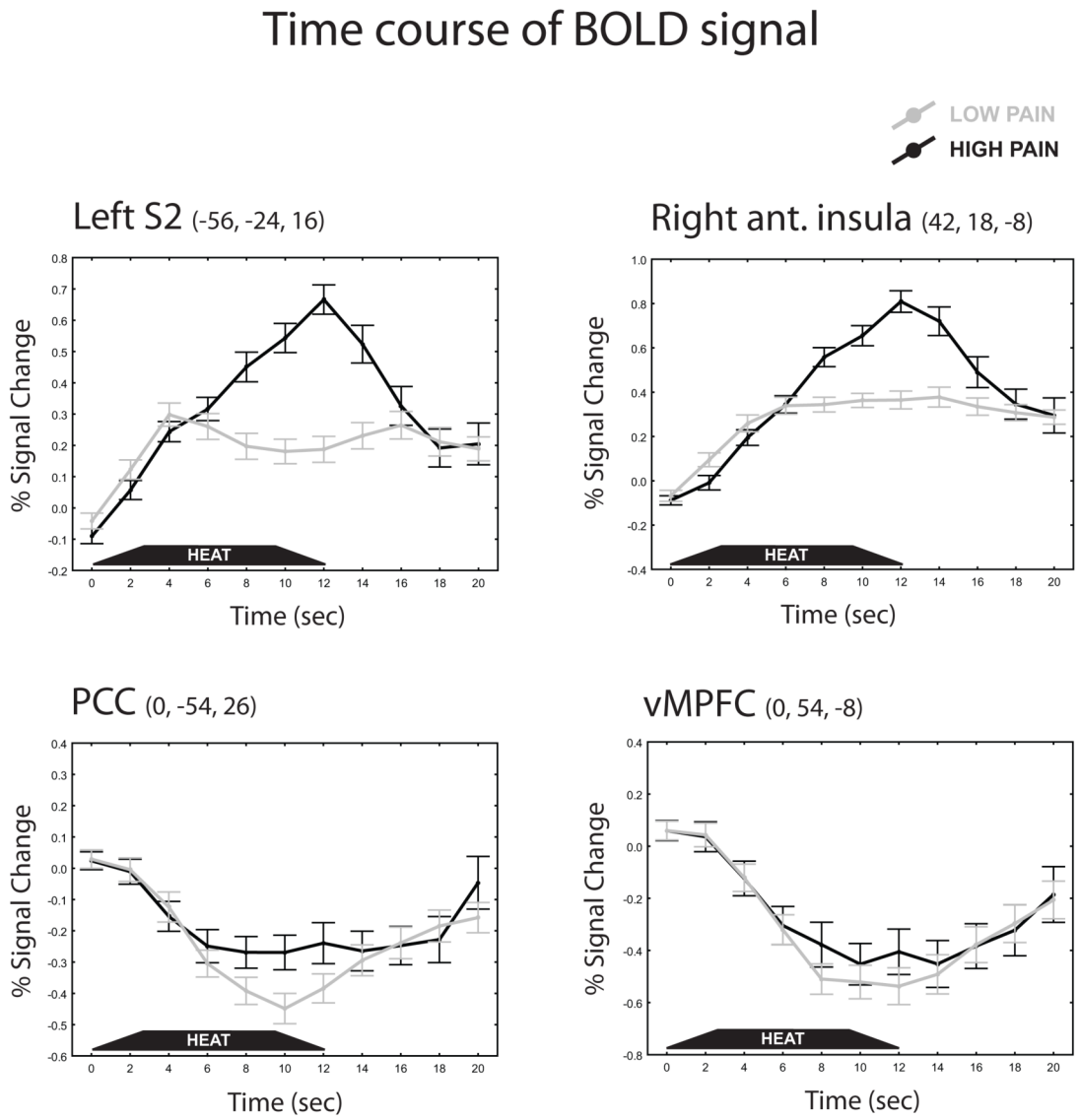


**Figure 2. Average time course of the BOLD signal within some exemplary pain-activated and –deactivated regions (average signal within 3mm spheres)**

The black trapezoids indicate the time of delivery of the 12 seconds of heat stimulation. Bars represent the standard error of the mean.

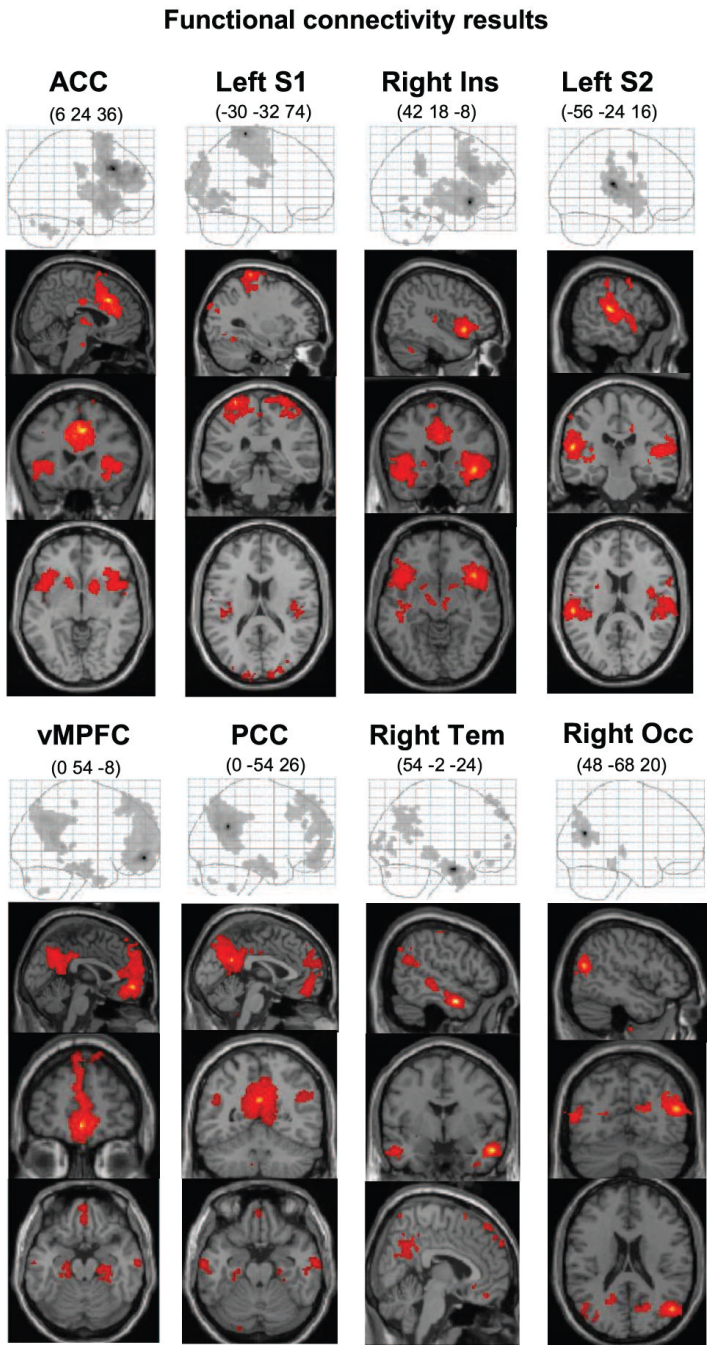


**Figure 3. Functional connectivity results during resting state**

Upper row shows the results for the areas displaying pain-evoked BOLD signal increase; lower row shows those for the areas displaying pain-evoked BOLD signal decrease.

## Table 1

fMRI signal changes evoked by LOW pain stimuli. For clusters extending over several anatomical areas, the first area listed represents the location of the (de)activation peak. Coordinates are in MNI space

| Comparisons | Area (Brodmann Area) | Z score | Number of voxels in cluster | Peak coordinate (x,y,z) |
|---|---|---|---|---|
| **fMRI signal increases (pain > baseline)** | Right insula | 7.29 | 2927 | 40 20 −6 |
| | Right inferior / middle frontal gyrus (45, 46, 10) | 6.83 | | 42 46 4 |
| | Left anterior insula | 6.75 | 445 | −34 16 −4 |
| | Left posterior insula | 6.2 | 171 | −40 −18 18 |
| | Bilateral medial frontal gyrus (8) | 5.89 | 156 | 6 26 48 |
| | Left S2 (2 / 43) | 5.35 | 32 | −64 −20 24 |
| | Right inferior parietal lobule (40) | 5.13 | 20 | 58 −42 52 |
| | Right middle frontal gyrus (9) | 4.98 | 37 | 52 18 34 |
| | Left cerebellum | 5.36 | 78 | −28 −66 −38 |
| **fMRI signal decreases (pain < baseline)** | Right lateral occipital gyrus / middle temporal gyrus / inferior parietal lobule (19 /18 / 39 / 21 / 40) | Inf | 28081 | 48 −68 20 |
| | Left lateral occipital gyrus / middle temporal gyrus / inferior parietal lobule (19 / 18 / 39 / 21 / 40) | Inf | | −30 −82 20 |
| | Bilateral precuneus / cingulate cortex / medial prefrontal cortex / paracentral lobule (7 / 23 / 31 / 6 / 4) | 7.64 | | −4 −36 46 |
| | Bilateral posterior cingulate / retrosplenial cortex (26 / 29 / 30 / 31 / 23) | 7.31 | | 0 −54 26 |
| | Right motor / premotor cortex (4 / 6) | 7.27 | | 46 −8 60 |
| | Left cerebellum | 7.28 | | −30 −40 −28 |
| | Right posterior thalamus | Inf | | 16 −26 0 |
| | Left posterior thalamus | 7.78 | | −14 −28 2 |
| | Left middle / inferior temporal gyrus (21 / 20) | 7.79 | 552 | −54 −4 −24 |
| | Left parahippocampus / hippocampus (35) | 6.18 | | −22 −4 −26 |
| | Left uncus (28) | 5.97 | | −34 −8 −30 |
| | Bilateral medial frontal gyrus / ACC / orbital prefrontal cortex (9,10, 32, 24 ,11) | 7.38 | 3590 | −4 64 28 |
| | Left superior frontal gyrus (8) | 6.46 | | −24 30 48 |
| | Right middle / inferior temporal gyrus (21 / 20) | 7.2 | 669 | 54 −2 −24 |
| | Right uncus / parahippocampus / hippocampus (28 / 35) | 5.5 | | 30 −6 −26 |
| | Left motor /premotor cortex (4 / 6) | 6.76 | 859 | −42 −12 48 |
| | Bilateral hypothalamus | 5.22 | 20 | −4 −2 −14 |
| | Right superior frontal gyrus (8) | 4.82 | 13 | 24 42 50 |

| Comparisons | Area (Brodmann Area) | Z score | Number of voxels in cluster | Peak coordinate (x,y,z) |
|---|---|---|---|---|
| | Left precentral gyrus (3) | 4.81 | 11 | −18 −24 64 |
| | Right cerebellum | 5.02 | 16 | 12 −46 −50 |
| | Right striatum | 4.97 | 23 | 28 −10 −2 |

## Table 2

fMRI signal change evoked by HIGH pain stimuli. See Table 1 caption

| Comparisons | Area (Brodmann Area) | Z score | Number of voxels in cluster | Peak coordinate (x,y,z) |
|---|---|---|---|---|
| **fMRI signal increases (pain > baseline)** | Right insula / operculum / inferior frontal gyrus (47) / thalamus / striatum / superior & middle temporal gyrus (12/ 21) | Inf | 33338 | 42 18 −8 |
| | Left insula / operculum / inferior frontal gyrus (47) / thalamus / striatum / superior & middle temporal gyrus (12 / 21) | Inf | | −40 −16 14 |
| | Left S2 (2 / 43 / 40) | Inf | | −56 −24 16 |
| | Right ACC / medial frontal gyrus (32/ 24 / 9) | 7.71 | | 6 24 36 |
| | Left ACC / medial frontal gyrus (32/ 24 / 9) | 7.46 | | −6 20 34 |
| | Right inferior / middle frontal gyrus (44 / 46 /10) | 7.29 | | 48 48 0 |
| | Right S2 (2 / 43 / 40) | 7.23 | | 56 −24 22 |
| | Left S1 / M1 (3 / 4) | 6.05 | | −30 −32 74 |
| | Left middle frontal gyrus (46 , 9) | 7.46 | 443 | −34 44 28 |
| | Bilateral brainstem | 6.03 | 23 | −2 −40 −48 |
| | Left cerebellum | 9.21 | 1379 | −34 −62 −32 |
| | Right cerebellum | 8.61 | 2376 | 26 −54 −30 |
| **fMRI signal decreases (pain < baseline)** | Right S1 / M1 (4 /3) | Inf | 861 | 44 −26 64 |
| | Bilateral medial prefrontal cortex / ACC (11 / 10 / 32 / 24) | 7.62 | 1250 | 0 34 −14 |
| | Bilateral posterior cingulate / precuneus (31 / 7 / 23 / 30) | 5.3 | 415 | 0 −50 32 |
| | Right lateral occipital gyrus (19) | 5.42 | 236 | 40 −78 30 |
| | Left lateral occipital gyrus (19) | 5.25 | 169 | −32 −82 28 |
| | Right superior parietal lobule (7) | 4.98 | 27 | 24 −70 60 |
| | Left superior frontal gyrus (8) | 4.92 | 15 | −12 50 40 |

## Table 3

Differences in the fMRI signal change evoked by HIGH pain and LOW pain stimuli. See Table 1 caption

| Comparisons | Area (Brodmann Area) | Z score | Number of voxels in cluster | Peak coordinate (x,y,z) |
|---|---|---|---|---|
| **HIGH pain > LOW pain** | Right insula / operculum / inferior frontal gyrus (47) / thalamus / striatum / superior / middle / inferior temporal gyrus (22 / 21/20) | Inf | 44376 | 38 8 6 |
| | Left insula / operculum / inferior frontal gyrus (47) / thalamus / striatum / superior / middle temporal / inferior temporal gyrus (22 / 21/20) | Inf | | −40 −18 14 |
| | Left ACC / medial frontal gyrus / paracentral lobule/midcingulate / posterior cingulate cortex / precunus (24 / 6 / 4 / 32 / 23 / 31) | Inf | | −4 6 42 |
| | Right ACC / medial frontal gyrus / paracentral lobule/ midcingulate / posterior cingulate cortex / precunus (24 / 6 / 4 / 32 / 23 / 31) | Inf | | 6 18 36 |
| | Left S2 / inferior parietal lobule (2 / 43 / 40) | Inf | | −58 −30 22 |
| | Right S2 / inferior parietal lobule (2 / 43 / 40) | 7.11 | | 60 −34 24 |
| | Left M1 /premotor area / S1 (4 / 6 / 3 / 1) | 6.61 | | −18 −26 60 |
| | Left cerebellum | 6.62 | | −30 −52 −36 |
| | Right cerebellum | 7.54 | | 26 −54 −30 |
| | Bilateral PAG | 6.33 | | −4 −24 −14 |
| | Left middle frontal gyrus (9) | 6.24 | 191 | −38 46 32 |
| | Right superior frontal gyrus (9) | 6.06 | 142 | 28 58 32 |
| | Right precentral gyrus (4 / 6) | 4.91 | 16 | 22 −26 60 |
| | Right premotor cortex (6) | 5.77 | 218 | 54 2 42 |
| | Left medial prefrontal cortex (9) | 4.94 | 14 | −6 56 24 |
| | Left middle temporal gyrus (39) | 4.99 | 21 | −48 −52 12 |
| | Right middle temporal gyrus (21) | 5.48 | 39 | 48 −40 −2 |
| | Left calcarine sulcus / cuneus / middle occipital gyrus (17 /18 / 19) | 5.28 | 251 | −20 −70 10 |
| | Left cuneus (19) | 4.95 | 86 | −8 −82 32 |
| | Right cuneus (19) | 4.88 | 33 | 16 −70 32 |
| | Left cerebellum | 4.79 | 12 | −18 −52 −16 |
| **LOW > HIGH** | No region above the set threshold | | | |

**Table 4**

Pearson correlation between fMRI signal changes evoked by LOW pain. Peak MNI coordinates (x, y, z) used for beta value extraction are displayed. In each cell the correlation coefficient r and, between brackets, the p value are indicated. Significant correlation after Bonferroni correction (p=0.05/55 =0.0009) are marked in bold

| | **LOW pain fMRI signal increases** | | | **LOW pain fMRI signal decreases** | | | | | | | |
|---|---|---|---|---|---|---|---|---|---|---|---|
| | **Left insula (−34 16 −4)** | **Right insula (40 20 −6)** | **Left S2 (−64 −20 4)** | **Left Occ. G. (−30 −82 20)** | **Right Occ. G. (48 −68 20)** | **PCC (0 −54 26)** | **vMPFC (0 54 −8)** | **dMPFC (−4 64 28)** | **Left Tem G (−54 −4 −24)** | **Right Tem G (54 −2 −24)** | **Precuneus (−4 −36 46)** |
| Left insula | 1.00 | **0.69 (<0.0001)** | **0.43 (0.0005)** | 0.15 (0.24) | 0.09 (0.51) | 0.19 (0.14) | 0.22 (0.08) | 0.22 (0.1) | 0.21 (0.1) | 0.14 (0.29) | 0.31 (0.02) |
| Right insula | | 1.00 | **0.48 (<0.0001)** | 0.07 (0.58) | −0.14 (0.30) | 0.06 (0.65) | 0.05 (0.71) | −0.02 (0.89) | 0.06 (0.64) | 0.09 (0.48) | 0.14 (0.28) |
| Left S2 | | | 1.00 | 0.36 (0.004) | 0.19 (0.14) | 0.11 (0.42) | 0.19 (0.14) | −0.00 (0.99) | 0.18 (0.16) | 0.18 (0.17) | 0.24 (0.07) |
| Left Occ. G. | | | | 1.00 | **0.56 (<0.0001)** | 0.19 (0.15) | 0.32 (0.01) | 0.23 (0.08) | 0.39 (0.002) | 0.20 (0.12) | 0.37 (0.003) |
| Right Occ. G. | | | | | 1.00 | **0.44 (0.0004)** | **0.66 (<0.0001)** | 0.27 (0.03) | **0.54 (<0.0001)** | **0.42 (0.0009)** | **0.53 (<.0001)** |
| PCC | | | | | | 1.00 | **0.77 (<0.0001)** | **0.51 (<0.0001)** | **0.51 (<0.0001)** | **0.60 (<0.0001)** | **0.59 (<.0001)** |
| OMPFC | | | | | | | 1.00 | **0.58 (<0.0001)** | **0.61 (<0.0001)** | **0.70 (<0.0001)** | **0.54 (<.0001)** |
| VMPFC | | | | | | | | 1.00 | **0.49 (<0.0001)** | **0.45 (0.0003)** | **0.54 (<.0001)** |
| Left Lat Temp. C. | | | | | | | | | 1.00 | **0.76 (<0.0001)** | **0.55 (<.0001)** |
| Right Lat Temp. C. | | | | | | | | | | 1.00 | **0.49 (<.0001)** |
| Precuneus | | | | | | | | | | | 1.00 |

**Table 5**

Pearson correlation between fMRI signal changes evoked by HIGH pain. See Table 4 caption

| | **HIGH pain fMRI signal increases** | | | | | | **HIGH pain fMRI signal decreases** | | | | |
|---|---|---|---|---|---|---|---|---|---|---|---|
| | **Left insula (−36 10 0)** | **Right insula (42 18 −8)** | **Left S2 (−56 −24 16)** | **Right S2 (56 −24 22)** | **Left S1 (−30 −32 74)** | **ACC (6 24 36)** | **Left Occ. G. (−32 −82 28)** | **Right Occ. G. (40 −78 30)** | **PCC (0 −50 32)** | **vMPFC (0 34 −14)** | **right S1/ M1 (44 −26 64)** |
| Left insula | 1.00 | **0.75 (<0.0001)** | **0.50 (<0.0001)** | **0.61 (<0.0001)** | **0.52 (<0.0001)** | **0.75 (<0.0001)** | 0.34 (0.008) | 0.33 (0.009) | 0.26 (0.05) | 0.03 (0.84) | 0.08 (0.52) |
| Right insula | | 1.00 | 0.39 (0.0019) | **0.47 (0.0001)** | **0.43 (0.0005)** | **0.68 (<0.0001)** | 0.23 (0.08) | 0.24 (0.07) | 0.12 (0.35) | −0.05 (0.68) | 0.09 (0.48) |
| Left S2 | | | 1.00 | **0.58 (<0.0001)** | **0.55 (<0.0001)** | **0.59 (<0.0001)** | 0.20 (0.13) | 0.17 (0.18) | 0.27 (0.04) | 0.23 (0.07) | 0.29 (0.02) |
| Right S2 | | | | 1.00 | **0.49 (<0.0001)** | **0.53 (<0.0001)** | 0.16 (0.21) | 0.14 (0.27) | 0.10 (0.46) | 0.11 (0.38) | 0.18 (0.16) |
| Left S1 | | | | | 1.00 | **0.65 (<0.0001)** | **0.54 (<0.0001)** | **0.47 (0.0001)** | 0..36 0.004 | 0.15 (0.25) | **0.50 (<0.0001)** |
| ACC | | | | | | 1.00 | 0.37 (0.004) | 0.35 (0.005) | 0.39 (0.002) | 0.12 (0.34) | 0.24 (0.08) |
| Left Occ. G. | | | | | | | 1.00 | **0.74 (<0.0001)** | **0.53 (<0.0001)** | 0.27 (0.03) | 0.39 (0.002) |
| Right Occ. G. | | | | | | | | 1.00 | **0.53 (<0.0001)** | 0.25 (0.06) | 0.38 (0.0023) |
| PCC | | | | | | | | | 1.00 | **0.48 (<0.0001)** | 0.32 (0.01) |
| OMPFC | | | | | | | | | | 1.00 | 0.30 (0.02) |
| Right S1 | | | | | | | | | | | 1.00 |

## Table 6

Brain regions and peak MNI coordinates (x, y, z) for functional connectivity analysis (3 mm sphere)

| **Seeds for fMRI signal increase** | | **Seeds for fMRI signal decrease** | |
|---|---|---|---|
| **Brain region** | **Coordinate** | **Brain region** | **Coordinate** |
| Right insula | (42 18 −8) | vMPFC | (0 54 −8) |
| Left S2 | (−56 −24 16) | PCC | (0 −54 26) |
| Left S1 | (−30 −32 74) | Right Occ. G. | (48 −68 20) |
| Right ACC | (6 24 36) | Right Temp. Cx. | (54 −2 −24) |